Received: 4 December 2023 | Revised: 17 January 2024 | Accepted: 1 March 2024

DOI: 10.1002/bit.28697

ARTICLE

BIOTECHNOLOGY AND BIOENGINEERING WILEY

Transport-controlled growth decoupling for self-induced protein expression with a glycerol-repressible genetic circuit

Alvaro R. Lara[1] | Flavio Kunert[2] | Vincent Vandenbroucke[3] | Hilal Taymaz-Nikerel[4] | Luz María Martínez[5] | Juan-Carlos Sigala[6] | Frank Delvigne[3] | Guillermo Gosset[5] | Jochen Büchs[2]

[1]Department of Biological and Chemical Engineering, Aarhus University, Aarhus, Denmark

[2]Biochemical Engineering (AVT.BioVT), RWTH Aachen University, Aachen, Germany

[3]Terra Research and Teaching Centre, Microbial Processes and Interactions (MiPI), Gembloux Agro-Bio Tech, University of Liège, Gembloux, Belgium

[4]Department of Genetics and Bioengineering, Istanbul Bilgi University, Istanbul, Turkey

[5]Instituto de Biotecnología, Universidad Nacional Autónoma de México, Cuernavaca, México

[6]Departamento de Procesos y Tecnología, Universidad Autónoma Metropolitana, Ciudad de México, México

Correspondence

Alvaro R. Lara, Department of Biological and Chemical Engineering, Aarhus University, Gustav Wieds Vej 10, 8000 Aarhus, Denmark.
Email: alvaro.lara@bce.au.dk

Funding information

Consejo Nacional de Humanidades, Ciencias y Tecnologías; Exploratory Research Space RWTH Aachen University; CONAHCyT, Grant/Award Number: A1-S-8646

Abstract

Decoupling cell formation from recombinant protein synthesis is a potent strategy to intensify bioprocesses. *Escherichia coli* strains with mutations in the glucose uptake components lack catabolite repression, display low growth rate, no overflow metabolism, and high recombinant protein yields. Fast growth rates were promoted by the simultaneous consumption of glucose and glycerol, and this was followed by a phase of slow growth, when only glucose remained in the medium. A glycerol-repressible genetic circuit was designed to autonomously induce recombinant protein expression. The engineered strain bearing the genetic circuit was cultured in 3.9 g L^{-1} glycerol + 18 g L^{-1} glucose in microbioreactors with online oxygen transfer rate monitoring. The growth was fast during the simultaneous consumption of both carbon sources (C-sources), while expression of the recombinant protein was low. When glycerol was depleted, the growth rate decreased, and the specific fluorescence reached values 17% higher than those obtained with a strong constitutive promoter. Despite the relatively high amount of C-source used, no oxygen limitation was observed. The proposed approach eliminates the need for the substrate feeding or inducers addition and is set as a simple batch culture while mimicking fed-batch performance.

KEYWORDS

bioprocess intensification, C-source mixtures, genetic circuit, growth decoupling, microbial engineering

1 | INTRODUCTION

Cellular resources stewardship and allocation are key factors to be considered for bioprocess intensification. A promising strategy to optimize molecule synthesis in cultures is to decouple cell growth from product formation. This strategy aims at using the cellular resources for biomass formation, followed by a metabolic rearrangement to synthesize the desired product, while limiting the amount of biomass formation by an external factor, like a specific nutrient (Lo et al., 2016; Menacho-Melgar et al., 2020). More refined methods include the inhibition of cell division and host mRNA transcription by the viral protein Gp2, induced by L-arabinose.

Recombinant protein expression is then mediated by the T7 RNA polymerase, which is not affected by Gp2 (Stargardt, et al., 2020). Kasari et al. (2022) induced the removal of *oriC* from the chromosome of *Escherichia coli* by a site-specific serine recombinase, which stopped cell growth and was coupled to recombinant protein expression. Ideally, growth decupling schemes could be combined with the autonomous induction of protein expression by environmental factors like carbon source (C-source) (Bothfeld et al., 2017; Guo et al., 2022; Strittmatter, Egli, et al., 2021), shear rate (Strittmatter, Argast, et al., 2021), or dissolved gases (Werner et al., 2007) in high-cell density cultures. Attaining high cell-densities in batch mode remains a challenge, due to metabolic and physical constraints. The accumulation of toxic overflow metabolites and the oxygen demand by cells limit the amount of C-source that can be used in batch cultures. These can be overcome by fed-batch schemes. However, fed-batch cultures are more complex to operate, their implementation at a small scale in microtiter plates (MTPs) and shaking flasks is very limited, and the oxygen and C-source distribution in the liquid phase are usually heterogeneous in bioreactor scales above for example, 10 m^3 (Lara et al., 2006). A biological alternative is to decrease the glucose uptake rate by deleting genes that express proteins related to carbohydrate transport through the cell membranes. Glucose transport mutants of *E. coli* display strongly reduced overflow metabolism and can be cultured to high cell densities in batch mode, even if osmolality was as high as 1.6 Osm kg^{-1} (Lara et al., 2008). Such strategy allowed reaching attractive amounts of recombinant proteins or DNA vaccines (Borja et al., 2012; Velazquez et al., 2022). A particular mutant, named WGM (Δ*ptsG* Δ*manX*), can produce recombinant protein levels that are remarkably higher than those of its parental strain, while maintaining slow biomass formation (Fragoso-Jiménez et al., 2022; Velazquez et al., 2022). Furthermore, glucose transport mutants lack carbon catabolite repression (Martínez et al., 2008), which expands the possibilities for culture design (Fox & Prather, 2020). In this study, we used strain WGM to develop a culture scheme, in which cell growth is decoupled from recombinant protein expression by using a mixture of glycerol and glucose, in which glycerol availability controls the transition to slow biomass formation. A genetic circuit was designed to allow self-induction of recombinant protein expression upon glycerol depletion. This resulted in efficient growth decoupling and autonomous induction in a simple batch culture requiring no further intervention, like the addition of inducers or fed-batch operation.

2 | MATERIALS AND METHODS

2.1 | Strains

The K-12 derivative W3110 *E. coli* strain was used as wild type. Strain WGM is a Δ*ptsG* Δ*manX* derivative of W3110 (Fuentes et al., 2013). The *lacI* gene was further deleted in each strain. Both strains were transformed with the genetic circuits described below. Transformed and untransformed strains were plated in Petri dishes and grown at 37°C for 14–18 h. One colony per strain was selected and grown in Terrific Broth (TB) medium until reaching an optical density at 600 nm (OD_{600}) of approx. 6–8. Then, 0.9 mL of such culture broth was mixed with a sterile solution of glycerol (80% v/v) and immediately frozen at −80°C.

2.2 | Genetic circuits

A flavin mononucleotide-based fluorescent protein (FbFP) was employed as a reporter. A constitutive protein generator (CPG, 2405 bp) was designed to express the optimized *fbfp* gene (Lara, Jaén, Sigala, Mühlmann, et al., 2017; Lara, Jaén, Sigala, Regestein, et al., 2017) under transcriptional control of the P_{trc} promoter. The design lacks the *lacI* operator sequence. The architecture of the glycerol-repressible genetic circuit (GRC, 4721 bp) was inspired by the switch proposed by Gardner et al. (2000). The sequences were synthesized and cloned in the plasmid pUC57mini by GenScript. A more detailed description of the GRC is given in Section 3.3.

2.3 | Precultures development

All chemicals used for media preparation were of analytical grade and purchased from Carl Roth GmbH, if not stated otherwise. A first preculture was performed by transferring 0.05 mL of the cryopreserved cells to 8 mL of TB medium contained in a 250 mL Erlenmeyer flask. The composition of TB was (in g L^{-1}): yeast extract, 24; tryptone, 20; glycerol, 4. The cells were grown at 37°C and 350 rpm in an orbital shaker of 50 mm shaking diameter for 6 h. Next, 0.05 mL were transferred to 8 mL of mineral medium contained in a 250 mL Erlenmeyer flask and cultured at 30°C and 350 rpm in an orbital shaker of 50 mm shaking diameter until mid-exponential growth phase (approx. 14–16 h). The mineral medium composition was (in g L^{-1}): $(NH_4)_2SO_4$, 6.5; NH_4Cl, 0.5; K_2HPO_4, 3.0; Na_2SO_4, 2.0; $MgSO_4 \bullet 7H_2O$, 0.5; thiamine hydrochloride 0.01; MOPS, 41.85; plus 1 mL of trace elements solution per L of medium. Thiamine hydrochloride was purchased from Sigma-Aldrich. The initial pH was adjusted to 7.4 by adding NaOH 0.2 M. The presence of MOPS contributes to maintaining nearly neutral pH (Wewetzer et al., 2015). The media was autoclaved for sterilization. The trace elements solution was prepared and autoclaved separately. The composition of the trace element solution was (in g L^{-1}): $ZnSO_4 \bullet 7H_2O$, 0.54; $CuSO_4 \bullet 5H_2O$, 0.48; $MnSO_4 \bullet H_2O$, 0.30; $CoCl_2 \bullet 6H_2O$, 0.54; $FeCl_3 \bullet 6H_2O$, 41.76; $CaCl_2 \bullet 2H_2O$, 1.98; $Na_2EDTA \bullet 2H_2O$, 33.4. Glycerol was added at a final concentration of 10 g L^{-1}, before sterilization, except for precultures of WGM for characterization in shaking flasks with glucose as the only C-source. In this case, 10 g L^{-1} glucose was used in the second preculture. Glucose was added form a separately autoclaved solution at a concentration of 500 g L^{-1}. For all cultures of plasmid bearing cells, the media were supplemented with 0.1 g L^{-1} ampicillin sodium salt (purchased from Sigma-Aldrich). Aliquots from

the second preculture were washed with 0.9% sterile NaCl solution and used to inoculate the main cultures

2.4 | Cultures in shaking flasks

The untransformed strains were grown in 250 mL Erlenmeyer flasks containing 30 mL of the mineral medium plus glucose, glycerol, or both, at the concentrations explained in Section 3, at 37°C and 350 rpm in an orbital shaker of 50 mm shaking diameter. In parallel and using the same precultures and shaker, the oxygen transfer rates (OTR) were determined online using the Respiration Activity Monitoring System (RAMOS) (Anderlei et al., 2004) in independent flasks. In the RAMOS device, the OTR is measured in regular cycles in Erlenmeyer flasks that have been adapted with arms for gas inlet and outlet and a cap with oxygen sensors. A measuring cycle is comprised of two phases (Anderlei & Büchs, 2001). During the first phase (rinsing phase), air is continuously flushed at a rate adjusted such that the gas concentration in the headspace of the measuring flask is equivalent to that in the normal Erlenmeyer flask. During the second phase (measuring phase), inlet and outlet valves of the measuring flask are closed. Microbial respiration leads to a decrease in the partial pressure of oxygen in the headspace of the measuring flask. The partial pressures are monitored by an oxygen sensor. Assuming linear changes in the measuring phase, a computer calculates the OTR. After the measuring phase, the valves are opened again, and the next measuring cycle starts. Before each measuring phase, the sensors are calibrated using the known steady state gas composition to compensate for signal drift. All the cultures were carried out in triplicates.

2.5 | Cultures in microbioreactors

Microbioreactor cultures were carried out in the mineral medium in 48-round transparent bottom wells MTP (Beckman Coulter) with a liquid volume of 0.75 mL per well, an initial OD_{600} of 0.1 units, at 37°C, 1000 rpm and 3 mm shaking diameter (Climo-Shaker ISF1-X; Kuhner). The shaken monitoring system, named µRAMOS-BioLector combination, is in-house constructed. It enables the measurement of the OTR in every individual well of the MTP applying a similar concept than in the RAMOS device. A microfluidic cover that contains in total 96 pneumatic valves and 48 optical fibers, providing two valves and one optical fiber for each well, is placed on top of the MTP. The OTR is measured on each well based on the oxygen partial pressure and oxygen-dependent emission of fluorescence sensors (Flitsch et al., 2016). Additionally, synchronized online measurement of fluorescence and scattered light (ScL) are carried out on each well (Ladner et al., 2016). The MTPs were covered with a gas-permeable polyolefin sealing foil (HJ-Bioanalytik GmbH), to reduce evaporation and prevent contaminations. Cell growth was monitored by measuring the ScL intensity at a wavelength of 620 nm. The wavelengths for excitation and fluorescence emission of FbFP were 450 and 492 nm, respectively. Four to six cultures of each strain were run on each experiment. All the experiments were carried out in triplicate.

2.6 | Characterization of protein expression at single cell level using offline flow cytometry

Single-cell FbFP measurements were first performed with flask cultures to ensure the protein is bright enough to be measured and provide a baseline of the expected behavior of the strain. The flask cultures were performed overnight in 100 mL flasks containing 10 mL mineral medium supplemented with 5 g L^{-1} glucose, at 37°C and 150 rpm shaking frequency. They include: (1) A culture of wild-type W3110 untransformed, (2) a culture of the strain W3110 bearing the CPG, (3) a culture of the strain W3110 bearing the GRC induced with 1 mM IPTG, and (4) a culture of the strain W3110 bearing the GRC with 1.25 g L^{-1} glycerol in addition to the glucose. They were then measured in an Attune® NxT Acoustic Focusing Cytometer (Thermo Fisher Scientific). The fluorescence measurement used a blue laser (488 nm) with a green filter (530/30 nm). FbFP positive or negative cells were determined based on a threshold. It was based on the CPG measurements, by fitting a gaussian mixture model (three distributions) to the logarithm of the data and selecting the minimum of the fitted distribution, rounded to the 10th. This value was 230 (or $10^{2.36}$).

2.7 | Characterization of protein expression at a single cell level based on automated flow cytometry

The dynamic response of the GRC was characterized in stirred bioreactor cultures of strain W3110 coupled with automated flow cytometry. Precultures were grown from single colonies in LB, then 50 µL were cultured overnight in the mineral medium supplemented with 5 g L^{-1} glucose. The main cultures were carried out in a DASbox® Mini Bioreactor System (Eppendorf) with 150 mL liquid volume, 1 vvm aeration rate, 1000 rpm, pH 7 (as it was controlled, only 5 g L^{-1} of MOPS were used), and 37°C, with a starting OD adjusted to 0.1, in a medium containing 2 g L^{-1} glucose and 4 g L^{-1} glycerol to observe the phenotype switch. Every 12 min, a sample was automatically taken from the bioreactor and diluted for analysis (Sassi et al., 2019). The cells were analyzed in a flow cytometer (BD Accuri C6; BD Biosciences) with an FSCH analysis threshold of 20,000. The fluorescence is generated by excitation with a 488 nm laser and emission is recorded through a 530/33 nm filter. Three identical bioreactors were running in parallel and produced similar fluorescence profiles, apart from the initial fluorescence that depended on the preculture and quickly rose to similar values. The fluorescence threshold for FbFP positive or negative cells was based on visual analysis at the end of the culture, when the population becomes purely negative. While the exact value used is arbitrary (600 or $10^{2.78}$), variations between 550 and 650 show very little change in the proportion trends.

2.8 | Quantification of metabolites concentrations

Glucose, glycerol, and acetate were measured via a high-performance liquid chromatography system (Shimadzu Prominence LC-20) equipped with a precolumn Organic Acid Resin (40 × 8 mm; CS-Chromatographie Service), a separating column Organic Acid Resin (250 × 8 mm; CS-Chromatographie Service), and a refraction index detector RID-20A (Shimadzu). The flow rate of the mobile phase (5 mM H_2SO_4) was set to 0.8 mL min^{-1} with a column temperature of 50°C.

2.9 | Data analysis

The data from fluorescence and ScL intensities are represented as the corresponding reading minus the lowest reading (usually obtained during the first 20 min of culture). The specific fluorescence (SF) was calculated as the mean of the fluorescence divided by the ScL readings at every time point during the period involved. Specific yields and rates were calculated by the proper mass balances over the time periods involved. To calculate the specific consumption rates in cultures with simultaneous consumption of glucose and glycerol, the change of each C-source concentration over time was described by a polynomial fit. Next, the first derivative was calculated and divided by the biomass concentration for every data point and the average specific uptake rate was calculated. Statistically significant differences were determined by means of two-tails heteroscedastic *t*-Student tests with a confidence level of 95% ($\alpha = 0.05$).

2.10 | Flux balance analysis (FBA)

FBA was carried out using *E. coli* genome scale model (Orth et al., 2011) in COBRA toolbox (Schellenberger et al., 2011), maximizing biomass formation. For constraints of FBA, measured substrate uptake rates of glucose and glycerol, and production rate of acetate were implemented for both strains. For strain WGM, the flux of D-glucose transport via PEP:Pyr PTS (GLCptspp) was set to zero in all cases. In the presence of glycerol, ubiquinone-8-dependent glycerol-3-phosphate dehydrogenase (G3PD5) was used in the model. Additionally, flux of glycerol dehydrogenase (GLYCDx) was set to zero, since it was reported that this reaction is utilized under anaerobic consumption of glycerol, but not aerobically (Gonzalez et al., 2008).

3 | RESULTS AND DISCUSSION

3.1 | Metabolic characterization of transport-controlled growth decoupling

The growth of the wild type and engineered strains in glucose-glycerol mixtures was characterized in shaking flasks with parallel online monitoring of the OTR. Figure 1 shows the cell growth, C-sources consumption, acetate accumulation, and OTR. Cultures of strain W3110 were carried out with 1.5 g L^{-1} glucose plus 1.5 g L^{-1} glycerol to show the diauxic behavior. Glucose is consumed first, with the concomitant production of acetate (Figure 1a). The OTR increased in parallel to glucose consumption, reaching a peak at glucose exhaustion, followed by a transient decrease and further increase, indicating glycerol consumption (Figure 1a,b). During the consumption of glycerol, acetate does not accumulate anymore (Figure 1a). The second OTR peak indicates the time of glycerol exhaustion, and a slow decrease of OTR corresponds to acetate assimilation. The diauxic growth is not clearly visible in Figure 1a, probably due to the relatively short time of growth on glycerol after glucose exhaustion. Also, the difference of the growth rates in

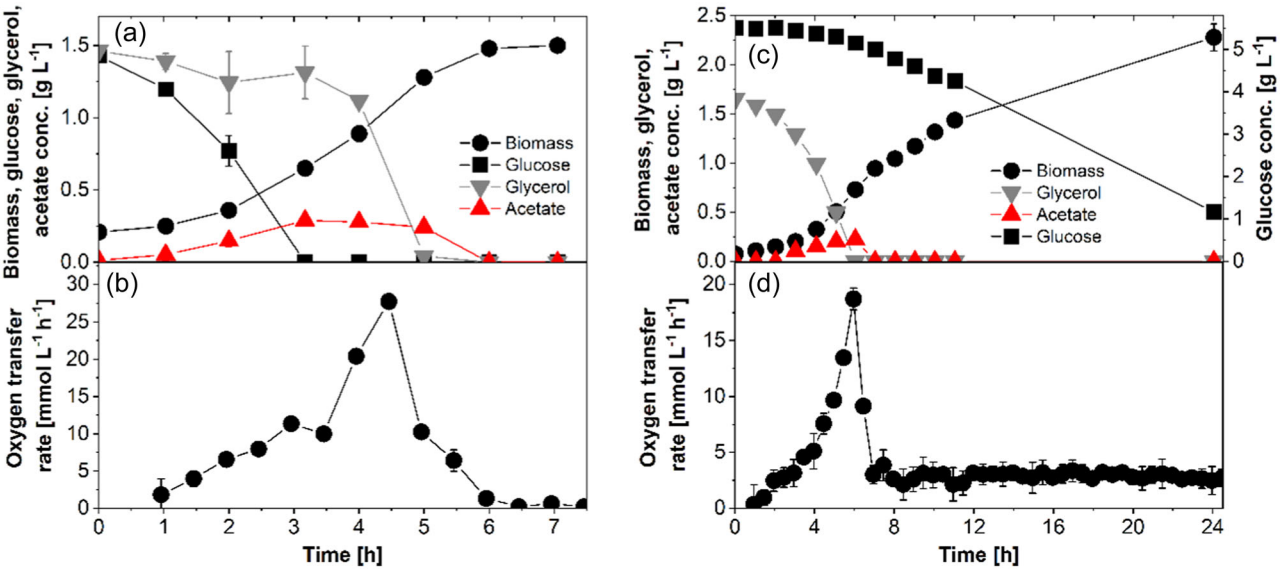

FIGURE 1 (a, b) Typical diauxic growth of the strain W3110 in a mixture of glucose and glycerol. (c, d) Transport-controlled growth decoupling in strain WGM in mixtures of glucose and glycerol.

glucose and glycerol is not too large for strain W3110 (explained in detail below). However, the C-source shift can be clearly tracked by the OTR signals, demonstrating the utility of these measurements to support metabolic engineering and synthetic biology studies. Strain WGM was cultured with 5 g L^{-1} glucose plus 1.5 g L^{-1} glycerol to illustrate its fed-batch-like performance, due to growth decoupling. Biomass formation is relatively fast while both C-sources are consumed simultaneously (Figure 1c), which is accompanied by a fast OTR increase (Figure 1d). A peak of the OTR curve corresponds to the time of glycerol exhaustion, after which the remaining glucose is consumed and biomass formation is slow, while OTR remains at values near to 2.2 mmol L^{-1} h^{-1}. These results show that the strain WGM can be used to perform batch cultures that mimic fed-batch behavior using mixtures of glucose and glycerol. The second growth phase is controlled by the glucose transport rate and the proper selection of C-sources concentrations allows to avoid oxygen limitation. Thus, the fed-batch phase is mimicked by a low glucose uptake flux, despite actual saturating glucose levels. This can be described as a C-source transport-controlled growth rate shift, that could be used for biotechnological purposes.

To better compare the behavior of the strains in the different C-source, cultures with only one C-source were carried out. The extracellular rates of the cultures during exponential growth are reported in Table 1. When glucose was the only C-source, the growth rate (μ) and glucose uptake rate ($q_{glucose}$) of strain WGM were considerably lower than those of W3110 and produced no acetate ($q_{acetate} = 0$). When glycerol was the only C-source, strain WGM consumed it slower, but produced more acetate than strain W3110. In contrast, when both C-sources were present, the growth rate of WGM almost equaled that of W3110 but produced acetate at a lower rate than W3110 under the same conditions. The presence of glycerol did not affect the $q_{glucose}$ of W3110. However, in the case of strain WGM, both $q_{glucose}$ and $q_{glycerol}$ were lower than the values in cultures using only one C-source.

While the consumption rates of glucose and glycerol in mixtures decreased for strain WGM, compared to cultures using only one C-source, the total carbon uptake was very similar to the uptake of glycerol as the only C-source. This is well in agreement with the study of Okano et al. (2020), who proposed that in C-sources mixtures simultaneously consumed by *E. coli*, the glycerol uptake rate responds to the total carbon uptake flux, which remains at a level corresponding to that of growth on glycerol alone. After glycerol was totally consumed, strain WGM continued growing and consuming glucose at rates lower than those observed using only glucose (Table 1). The reason for this remains unclear. There are no limitations of other components in the culture medium, the pH was measured and probed to be 7.1 units, while oxygen was clearly non-limiting. Therefore, the slow growth rate after glycerol depletion could be related to biological memory, because the preculture was grown in glycerol for cultures in C-sources mixtures. We observed that, when glycerol was used in the precultures, the adaptation of the WGM strain for growth in glucose as the only C-source took more than 6 h (data not shown).

To better understand the physiological changes originated by the mutation and C-source availability, FBA was performed using a genome scale model. Four scenarios were evaluated: growth of strain W3110 in glucose, growth of strain WGM in glucose, the mixture of glucose and glycerol, and the growth of WGM in glucose after glycerol depletion. The results were normalized to the glucose uptake rate of each strain and condition, and are depicted in Figure 2.

When growing in glucose, the normalized fluxes to the pentose phosphate pathway (PPP) were lower in the strain WGM (Figure 2b) than in strain W3110 (Figure 2a). In strain W3110, the normalized carbon fluxes in the tricarboxylic acid cycle (TCA) were high from fumarate to alpha ketoglutarate (aKG), but slow from this compound to fumarate. Fumarate is formed from aKG by two reactions, which produce reduced electron transporters that are oxidized in the electron transport chain. The normalized low fluxes of these

TABLE 1 Extracellular rates of strains W3110 and WGM growing in glucose and glycerol, individually and in mixtures. All the rates were calculated during the exponential growth phase.

C-source	Strain	μ (h^{-1})	$q_{glucose}$ (mmolC g^{-1} h^{-1})	$q_{glycerol}$ (mmolC g^{-1} h^{-1})	$q_{acetate}$ (mmolC g^{-1} h^{-1})
Glucose	W3110	0.53 ± 0.02	45.0 ± 14.0	–	5.7 ± 1.3
	WGM	0.24 ± 0.01	18.0 ± 0.3	–	0.0 ± 0.0
Glycerol	W3110	0.43 ± 0.02	–	67.1 ± 7.5	2.3 ± 0.0
	WGM	0.35 ± 0.01	–	37.5 ± 1.3	3.7 ± 0.0
Glucose + glycerol	W3110	0.46 ± 0.01	45.0 ± 5.7	–	8.7 ± 0.7
	WGM	0.41 ± 0.00	5.3 ± 3.3	29.6 ± 1.6	7.0 ± 0.3
Glucose, after glycerol depletion	WGM	0.10 ± 0.01	5.0 ± 0.7	–	0.0 ± 0.0

Note: The values of the all the corresponding parameters in each condition showed statistically significant difference between strains W3110 and WGM ($\alpha = 0.05$).

Abbreviations: μ, specific growth rate; q_{acet}, specific acetate production rate; $q_{glycerol}$, specific glycerol uptake rate; q_S, specific glucose uptake rate.

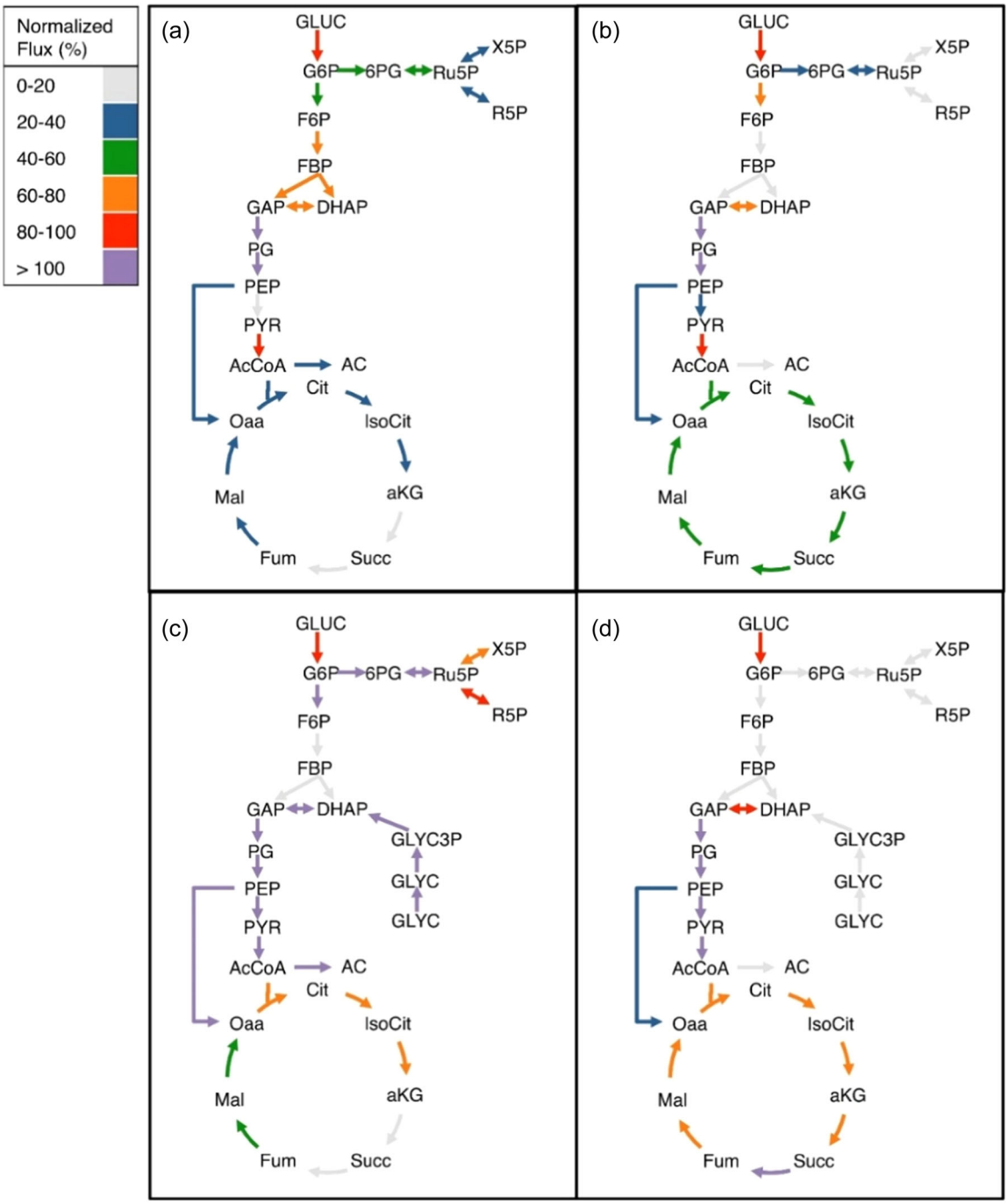

FIGURE 2 Metabolic fluxes of untransformed strains W3110 growing in glucose (a) and WGM growing in glucose (b), glycerol + glucose (c), and glucose after glycerol depletion (d). The fluxes are normalized to the value of $q_{glucose}$ in Table 1.

reactions, can be related to the limited respiratory capacity of the cells to fully oxidize the glucose transported at the maximum rate, thus originating overflow metabolites like acetate (Taymaz-Nikerel & Lara, 2021). This contrasts with the TCA normalized fluxes in WGM (Figure 2b), which displays similar rates in all the reactions. Such rates seem to be better balanced with the glycolytic rate of strain WGM because no overflow metabolism is present.

When glycerol and glucose are coutilized in strain WGM, the normalized carbon fluxes in the lower glycolysis increased. Similar to the growth of strain W3110 in glucose, the normalized fluxes from aKG to fumarate are low, with the result of acetate formation (Figure 2c). This effect has also been observed in chemostat cultures of *pts* knock-out strains (Yao et al., 2016). The transition from the coutilization of glycerol and glucose, to the consumption of glucose as the only C-source results in a low normalized carbon fluxes in the upper glycolysis and the PPP, while the normalized carbon fluxes in the whole TCA remained high, and acetate is not produced (Figure 2d). The low normalized carbon fluxes in the PPP and the

relatively fast formation of fumarate from succinate suggest a high energy demand and coincide with the low biomass formation. This may be an effect of the adaptation of growth using glucose as the only C-source after the utilization of glycerol.

3.2 | Expression of recombinant protein using glucose, glycerol, or mixtures in microbioreactors

FbFP was expressed in both strains using the CPG with glucose, glycerol, and mixtures in microbioreactor cultures. The amounts of C-source were selected to avoid oxygen limitation and to be able to observe growth decoupling in strain WGM. The μRAMOS-BioLector combination allowed characterizing the biomass growth and protein expression, while inferring the use of C-sources from the OTR data. The cultures profiles are shown in Figure 3.

Biomass formation was higher in glycerol than in glucose or mixtures for strain W3110 (Figure 3a), however, FbFP expression in glycerol was the lowest (Figure 3c). While the FbFP fluorescence increased constantly until reaching a plateau in cultures with only one C-source, there was a clear biphasic behavior in the case of C-source mixtures (Figure 3c). This correlates with the continuous OTR increase in the case of cultures in glucose, where a small second peak is observed after glucose exhaustion. It corresponds to the assimilation of acetate (Wewetzer et al., 2015). No second peak was observed in the case of cultures in glycerol, which can be related to lower acetate production using this C-source (Wewetzer et al., 2015, Table 1). When both C-source were present, the OTR peak corresponding to glucose exhaustion was observed shortly before 7 h of culture, while the peak corresponding to glycerol exhaustion close to the 10 h of culture (Figure 3e). The shift in C-source perturbed the FbFP expression, although the final fluorescence values reached that of cultures in glucose, while the final FbFP fluorescence was the lowest for cultures in glycerol (Figure 3c).

As expected, growth of strain WGM in glucose was slow (Figure 3b), and even though it reached the same final ScL signal as W3110, the FbFP fluorescence was 9% lower than for the parental strain (Figure 3c,d). Similar to the results of strain W3110, when growing in glycerol, strain WGM produced more biomass than in glucose (Figure 3b), but lower FbFP expression (Figure 3d). When strain WGM was grown in a mixture of glucose and glycerol, two growth phases were observed again, first a fast growth phase that correspond to simultaneous consumption of glycerol and glucose, followed by slow growth in glucose as the only C-source, as evidenced by the OTR curve (Figure 3b,f). The increase of FbFP fluorescence was also affected by the availability of C-sources, shifting from an exponential increase to a linear increase phase. The final FbFP fluorescence reached by strain WGM in the C-source mixture was 41% higher than in glycerol, but 16% lower than in glucose as the only C-sources.

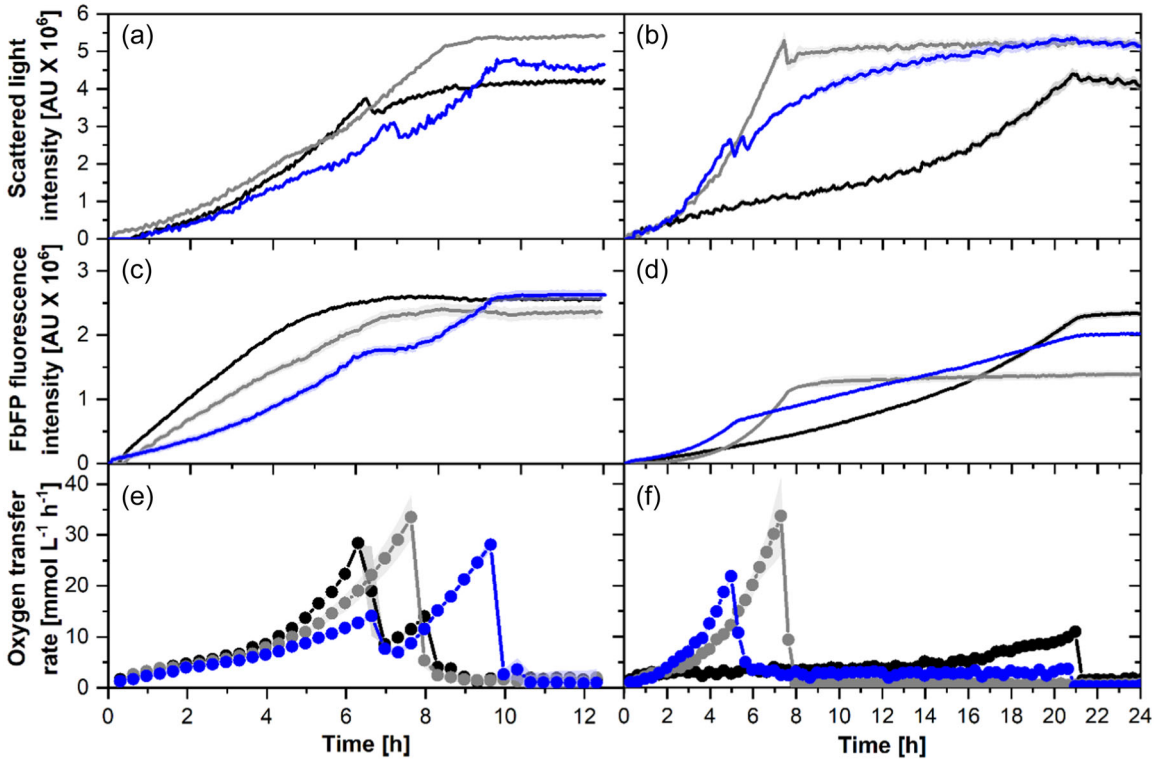

FIGURE 3 Growth profiles of strains W3110 (left panel) and WGM (right panel) bearing the CPG in 4 g L^{-1} glucose (black lines), 4 g L^{-1} glycerol (gray lines), or 2.5 g L^{-1} glucose + 1.5 g L^{-1} glycerol (blue lines). Data represent the average of four cultures. Shaded bands indicate the standard deviation between replicates. CPG, constitutive protein generator. (a, b) Scattered light intensity; (c, d) FbFP fluorescence intensity; (e, f) oxygen transfer rate.

The specific growth rates (μ) and biomass specific FbFP fluorescence (SF, calculated as the slope of FbFP fluorescence vs. ScL intensity) during exponential growth are reported in Table 2. The SF were higher in glucose than in glycerol for both strains, and the growth rate of strain WGM was strongly increased when the C-source mixture was used, compared to growth using only glucose, but the SF fell to values similar to those in cultures using only glycerol. Nevertheless, after glycerol depletion, the SF increased for strain WGM to the values observed during growth in glucose as the only C-source. Taken together, these results point to the fact that glycerol of the mixture of glycerol and glucose is the best option to accumulate biomass, while glucose is the best C-source for FbFP expression. This contrasts with earlier autoinduction systems, in which glucose is used for cell growth, while protein expression is performed, after glucose depletion, in a mixture of lactose (as inducer) and glycerol (as the main C-source) (Li et al., 2011; Studier, 2005). Moreover, the reduced glucose uptake capacity of strain WGM did not reduce its capacity to express recombinant protein using glucose as the C-source.

TABLE 2 Specific growth rate (μ) and biomass specific fluorescence (SF) of the different strains bearing the CPG during exponential growth in glucose, glycerol of mixtures.

C-source	Strain	μ (h^{-1})	SF (AU AU^{-1})
Glucose	W3110	0.48 ± 0.01	0.58 ± 0.01
	WGM	0.09 ± 0.01	0.60 ± 0.01
Glycerol	W3110	0.35 ± 0.01	0.21 ± 0.01*
	WGM	0.41 ± 0.02	0.20 ± 0.01*
Glucose + glycerol	W3110	0.41 ± 0.01	0.50 ± 0.01
	WGM	0.45 ± 0.03	0.18 ± 010
Glucose, after glycerol depletion	WGM	0.09 ± 0.01	0.65 ± 0.03

Abbreviation: CPG, constitutive protein generator.

The values of the all the corresponding parameters in each condition showed statistically significant difference between strains W3110 and WGM ($\alpha = 0.05$), except for those marked with *. In that case, the significant difference is proved with $\alpha = 0.10$.

To further explore the potential of strain WGM to mimic fed-batch performance in batch mode, cultures using higher amounts of C-sources were performed. The profiles of cultures of strains W3110 and WGM bearing the CPG, using 10 g L^{-1} glucose + 3.6 g L^{-1} glycerol are shown in Figure 4. In cultures of strain W3110, the OTR reached a plateau at approx. 11 h of culture, which indicates oxygen limitation. Subsequently, the OTR decreases and further increases. This can be attributed to the consumption of fermentative by-products and glycerol. The strain WGM displayed a fed-batch like performance, achieving fast growth during the first 8 h of culture, followed by slow growth accompanied by linear increase of the FbFP fluorescence. The transport-controlled fed-batch performance was efficient to avoid any oxygen limitation. However, at the end of the cultures, both strains attained the same FbFP fluorescence levels (FL). Therefore, the advantages of strain WGM were combined with a genetic circuit to develop an autonomously inducible system as described in the next section.

3.3 | Glycerol-repressible genetic circuit

The results presented in previous sections show that the growth of strain WGM in glucose can be decoupled in dependence on the

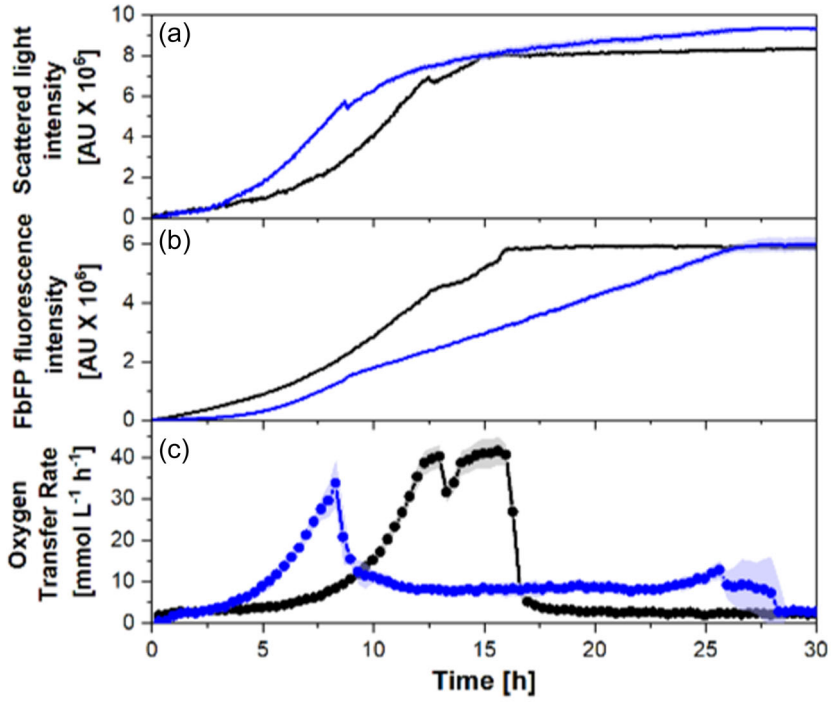

FIGURE 4 Growth profiles of strains W3110 (black lines) and WGM (blue lines) bearing the CPG in 3.6 g L^{-1} glycerol + 10 g L^{-1} glucose. Data represent the average of four cultures. Shaded bands indicate the standard deviation between replicates. CPG, constitutive protein generator. (a) Scattered ligth intensity; (b) FbFP fluorescence intensity; (c) oxygen transfer rate.

availability of glycerol. To make use of these growth characteristics for recombinant protein production, a system driving the expression of the gene of interest upon glycerol depletion is desirable. Initially, a promoter that seemed repressible by glycerol (Hemm et al., 2010) was tested, but the results were not satisfactory (data not shown). Therefore, a genetic circuit, designated as a GRC, was designed for the described purpose. The GRC is inspired by the switch proposed by Gardner et al. (2000), consisting of two promoters, each expressing the repressor of the other. A diagram of the GRC is shown in Figure 5a. The promoter P_{trc} controls the expression of the gene *glpR*, which codes for a repressor of the promoter P_{glpF}. In turn, P_{glpf} codes for *lacI*, which is the repressor of P_{trc}. The reporter gene *fbfp* is placed under transcriptional control of P_{trc}. While P_{trc} is inducible by IPTG, P_{glpF} is inducible by *sn*-glycerol 3-phosphate (G3P), which is formed from glycerol and ATP during the first reaction of glycerol dissimilation in *E. coli* (Lin, 1976). P_{glpF} controls the expression of the glycerol facilitator GlpF, a protein that allows the facilitated diffusion of glycerol across the inner membrane (Lin, 1976). The expression of GlpF is more than sevenfold greater in cultures using glycerol than in cultures using glucose as the C-source (Martínez-Gómez et al., 2012). A more detailed description of the circuit is given in the Supporting Information file. Figure 5b shows a representation of the GRC with logic gates. In total, there are four inputs, two of them can be considered internal (LacI and GlpR, expressed from the circuit itself), and two as externals: IPTG, which can be added to the medium, and G3P, which results from the presence of glycerol. Figure 5c shows the Boolean representation of the GRC, which should repress (OFF state), when glycerol is present, except in the case that IPTG is added.

Strain W3110 was transformed with the GRC and cultures under the conditions described in Figure 5c were carried out in micro-bioreactors and the SF was calculated during the exponential growth phase. The SF corresponding to each combination of external inputs is shown in Figure 5d. It should be noted that IPTG was used only to test the circuit. It is not to be used for other experiments, since autonomous induction is sought. As can be seen (Figure 5d), the GRC responded as expected, although the SF in the presence of glycerol and IPTG was slightly lower than in the case of glycerol absence (cultures in glucose). It is possible that a higher IPTG concentration is needed for complete induction of the circuit. The SF in the OFF state (cultures in glycerol and no IPTG addition), was approx. 20% of the ON state. This suggests that levels of *lacI* expressed from P_{glpF} are not

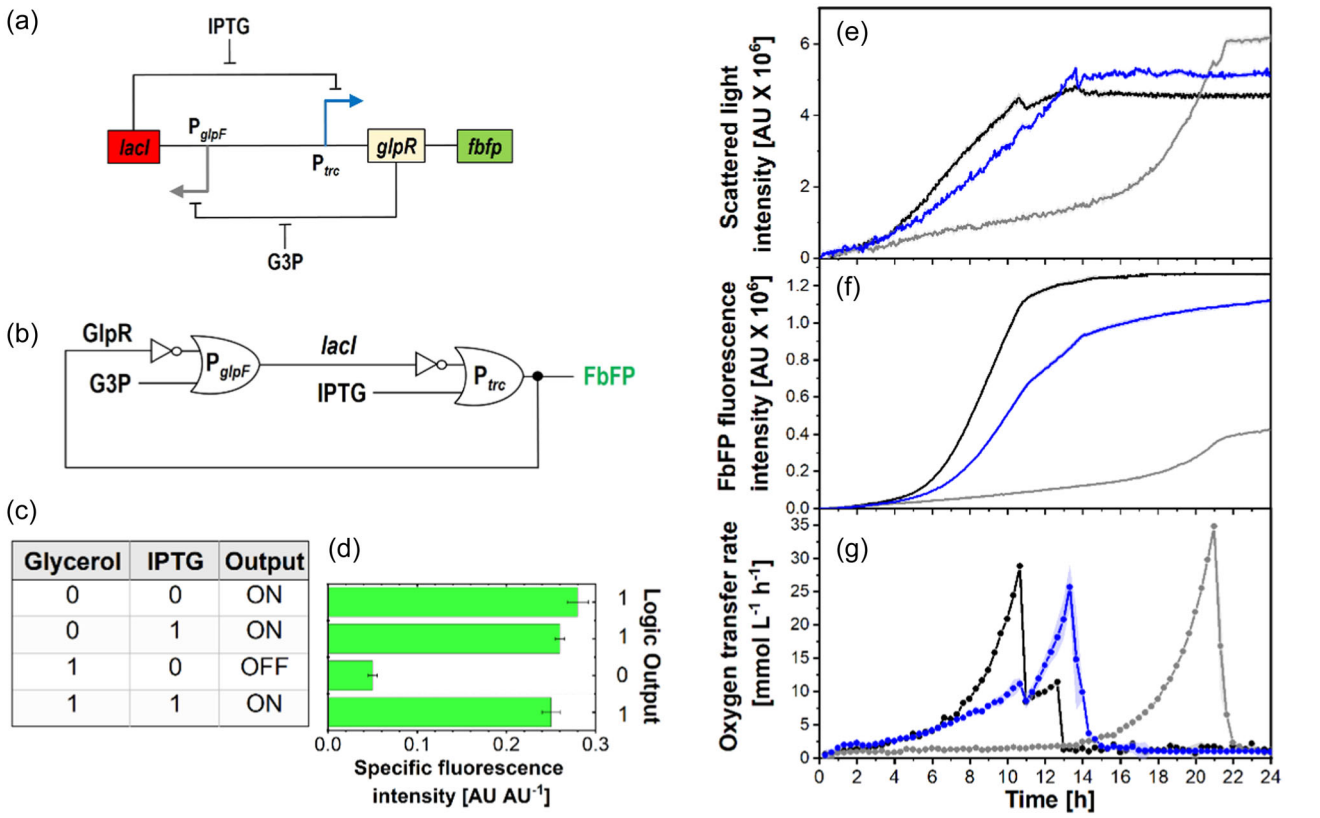

FIGURE 5 The glycerol-repressible genetic circuit (GRC). (a) Diagram of the circuit showing the arrangement of the promoters, inducers, and repressors. (b) Logic gates diagram of the GRC. (c) Boolean representation of the GRC. (d) Specific FbFP fluorescence (logic output) measured in cultures of strain W3110 bearing the GRC with glycerol or glucose as C-source, and with or without 0.1 mM IPTG addition. (e–g) Growth profiles of strain W3110 bearing the GRC in 4 g L^{-1} glucose (black lines), 4 g L^{-1} glycerol (gray lines), or 2.5 g L^{-1} glucose + 1.5 g L^{-1} glycerol (blue lines). No IPTG was added. Data represent the average of four cultures. Shaded bands (e–g) or error bars (d) indicate the standard deviation between replicates. FbFP, flavin mononucleotide-based fluorescent protein.

sufficient to completely repress P_{trc}, or that the levels of G3P are not high enough to inactivate GlpR. The SF in the ON state were lower than using the CPF in glucose (Table 2), despite the same promoter being used to control the expression of the FbFP. Factors like the burden associated with replication of a larger plasmid in the case of the GRP, or the coexpression of the GlpR repressor may have affected the expression of FbFP.

The growth, FbFP expression, and OTR profiles of strain W3110 bearing the GRC in glucose, glycerol, and mixtures are shown in Figure 5e–g. Similar to cultures using the CPG, biomass formation was the highest, when glycerol was the C-source, followed by the mixture of glycerol and glucose, and the lowest, when glucose was the only C-source (Figure 5e). In cultures using mixed C-sources, the FbFP fluorescence increased exponentially when glucose was consumed (SF = 0.28 ± 0.01 AU AU^{-1}) and decelerated when glycerol was the C-source (SF = 0.13 ± 0.01 AU AU^{-1}). This suggests that the GRC shifts to the OFF state, when the cells transit from glucose to glycerol consumption. The fact that the SF does not match the OFF state in Figure 5d can be explained by the fact that SF is affected by the low rate of FbFP expression in glycerol, but also by the FbFP that remains in the cells after expression in glucose.

To deepen the analysis of the cells' behavior, the GRC was analyzed at the single-cell level, first using off-line flow cytometry to verify how the different states manifest with the technique. As control, untransformed W3110 and the CPG-bearing strains were grown in shake flasks, and the cells were analyzed by flow cytometry using a blue laser (488 nm) with a green filter (530/30 nm). Figure 6a–c shows that it was possible to distinguish the population expressing FbFP from cells that are not expressing. A small fraction of the population (5%) bearing the CPG did not express the FbFP, and the fluorescent population had a median fluorescence of 1212 AU (Figure 6c). The same method was used to analyze cells bearing the GRC that should display OFF (culture at saturation induced with glycerol) or ON (glucose culture induced with IPTG) states, and the results are shown in Figure 6d–f. The exact fluorescence intensity depends on a number of factors that were not investigated at this point, such as the timing, repressor concentration, or the initial inoculum quantity and state. Nevertheless, it was possible to observe clear differences between the states of the GRC. When repressed with glycerol there were still 33% of cells expressing FbFP with a median fluorescence of 569 AU (Figure 6d). In contrast, in the sample of cells in the ON state, 13% of the population did not emit FbFP fluorescence, and the fluorescent fraction had a median expression of 821 AU (Figure 6e). In consequence, there is an overlap in the probability density function of these samples (Figure 6f) and partially explains the previous observations of a lower SF obtained with the GRC, compared to the CPG. Further, these results indicate that the fluorescence emission of cells bearing the GRC and grown in glycerol, results from a fraction of the population that escapes from the circuit repression.

To acquire more details on this escape and the behavior of the cells growing with mixed C-sources, the dynamic response of the GRC to a shift from glucose to glycerol consumption was studied with automated flow cytometry in 150 mL stirred bioreactors (Sassi et al., 2019), following a batch culture provided with 4 g L^{-1} glycerol and 2 g L^{-1} glucose. The results are depicted in Figure 6g, with a heat map representing the amount of cells found at any given time and FL, while the black line shows the oxygen profile. The latter produces the expected results given previous results on this strain: at approx. 9 h of culture, a shift on the dissolved oxygen was observed, that can be attributed to glucose exhaustion. This is followed by a fast oxygen consumption until approx. 13 h, when all the carbon is exhausted. The left axis of Figure 6g indicates the FL1-A for the heat map, as a proxy of FbFP expression measured in the flow cytometer. It should be noted that, despite FL1-A measures essentially the same fluorescence as BL1-H (Figure 6a–f), the measurements were performed in different devices and are reported in AU, and thus are not directly comparable. The scatter density was normalized so that each flow cytometry measurement has the same weight, and a change in color indicates a change in the proportion of cells with a given fluorescence. It shows, in yellow, a high concentration of cells, or in blue, a low concentration of cells.

At the start of the culture, it can be observed by the rather narrow yellow region that the bulk of the cells display a relatively high fluorescence, indicating glucose consumption, although the exact starting point of the preculture was not uniform across replicates. Over time, a fraction of the cells starts to display lower fluorescence, and after 6 h there is a clearly distinguishable fraction with a low FL. This occurs before the total glucose consumption (deduced from the dissolved oxygen shift at approx. 9 h). While the maximum fraction of positive cells varied between replicates between 50% and 70%, depending on the preculture starting point, it decreased uniformly across replicates and converged toward 7.2% positive cells (mean measurement of the last two measurements of the three replicates, with a standard deviation of 0.6%).

The activity of the P_{glpF} promoter depends on the G3P pool, but also on the cAMP-Crp complex (Okano et al., 2020). The GRC used in this study included four regions, upstream P_{glpF} (Supporting Information file). In a second version of the circuit, those sequences were removed, but FbFP expression was unsensitive to the C-source used (data not shown). Therefore, it can be expected that the cAMP-Crp complex pool will affect the GRC. It was shown that the cAMP-Crp complex pool is a function of the glucose uptake rate (You et al., 2013) and probably sensitive to the carbon uptake rate (Okano et al., 2020). The affinity for glucose is heterogeneous in cultures of *E. coli* (Smaluch et al., 2023), and thus q_{gluc} can also vary from cell-to cell. Overall fitness is also heterogeneous in bacterial cultures (Henrion et al., 2023). Therefore, the heterogenous FbFP expression observed in Figure 6f could have originated from the heterogeneity of glucose uptake and cAMP-Crp complex pool in the population.

3.4 | Transport-controlled growth decoupling with self-induced recombinant protein expression

The GRC was evaluated in the strain WGM in cultures with 3.8 g L^{-1} glycerol plus 18 g L^{-1} glucose in microbioreactors. These amounts of

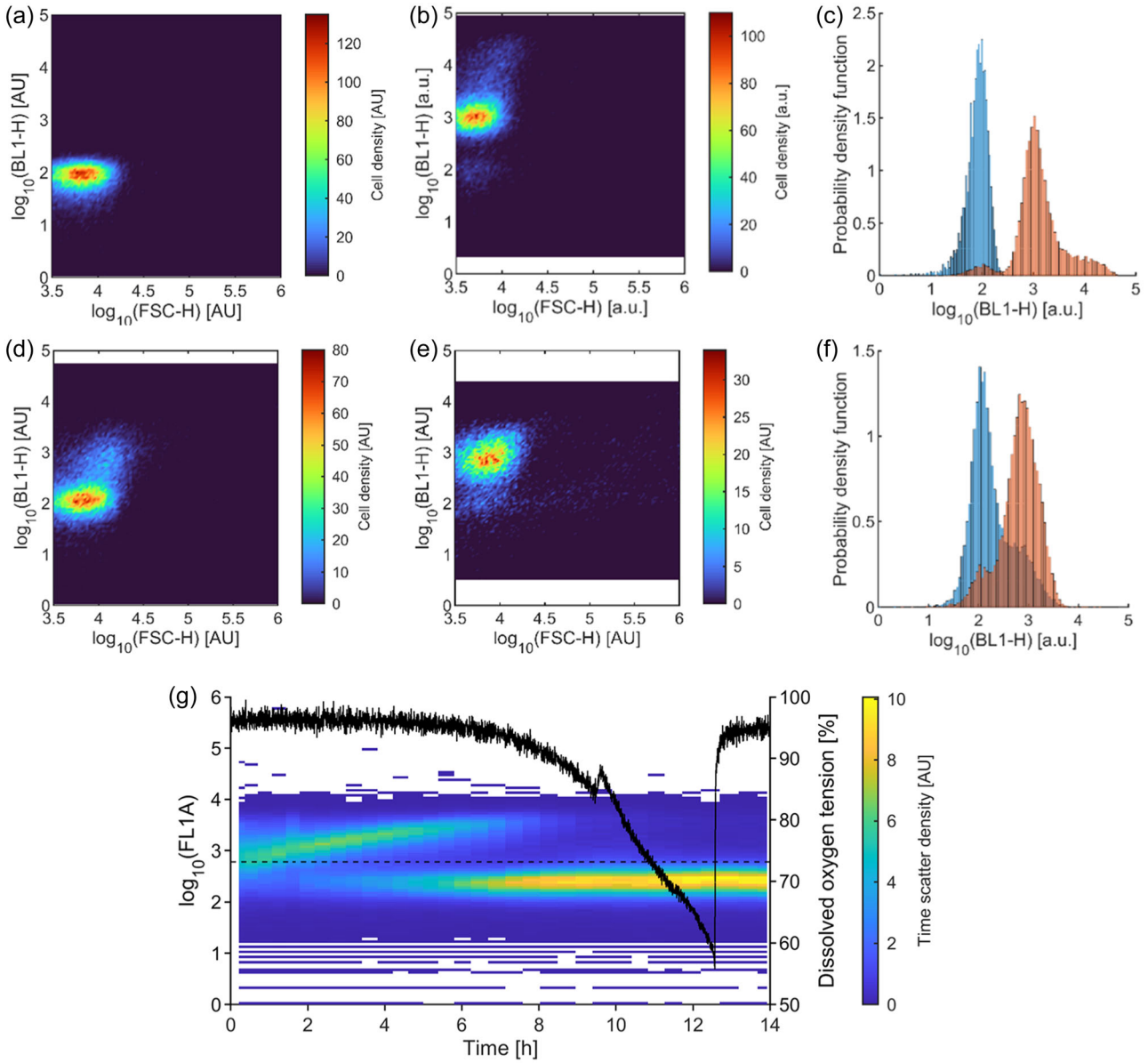

FIGURE 6 Characterization of the GRC at single-cell level in strain W3110. (a–e) Flow cytometry measurements of shaking flasks cultures. The forward scatter intensity (FSCH) is used as a proxy for cell size, while the fluorescence measurement for a blue laser (BL1-H) is used as a proxy for FbFP presence. (a) Measurement of untransformed strain grown in 5 g L^{-1} glucose until stationary phase. (b) Measurement of strain bearing the CPG grown in 5 g L^{-1} glucose until stationary phase. (c) Probability density function of untransformed cells (blue) and bearing the CPG (red). (d) Measurement of strain W3110 bearing the GRC grown in 5 g L^{-1} glucose and 1.25 g L^{-1} glycerol until stationary phase. (e) Measurement of strain W3110 bearing the GRC grown in 5 g L^{-1} glucose + 1 mM IPTG until stationary phase. (f) Probability density function of the cells bearing the GRC, repressed with glycerol (blue) and induced with IPTG (red). (g) Automated flow cytometry measurements of stirred mini bioreactor cultures of strain W3110 bearing the GRC in 4 g L^{-1} glycerol + 2 g L^{-1} glucose. Fluorescence measurements FL1A, shown by the heat map, are used to detect FbFP; the black line shows the oxygen profile. The dashed horizontal line shows the threshold used for determination of the fluorescent fraction. CPG, constitutive protein generator; FbFP, flavin mononucleotide-based fluorescent protein; GRC, repressible genetic circuit.

C-sources were used to increase the achievable biomass, while avoiding oxygen limitation. The culture profiles are shown in Figure 7. Consistent with the previous cultures, the strain WGM grew relatively fast during the co-consumption of glycerol and glucose, until approx. 11 h. At this point, the OTR reached a maximum of 43 mmol L^{-1} h^{-1} and then dropped, indicating glycerol exhaustion (Figure 7a). The presence of glycerol efficiently decoupled growth from FbFP expression, since the FbFP signal was considerably low during this culture phase (Figure 7a). The SF was calculated over this period, and remained at approx. 0.04 AU AU^{-1}, which was lower than the SF of strain W3110 growing in glycerol (Figure 5d). This indicates that both C-sources are used to synthesize biomass preferably, while

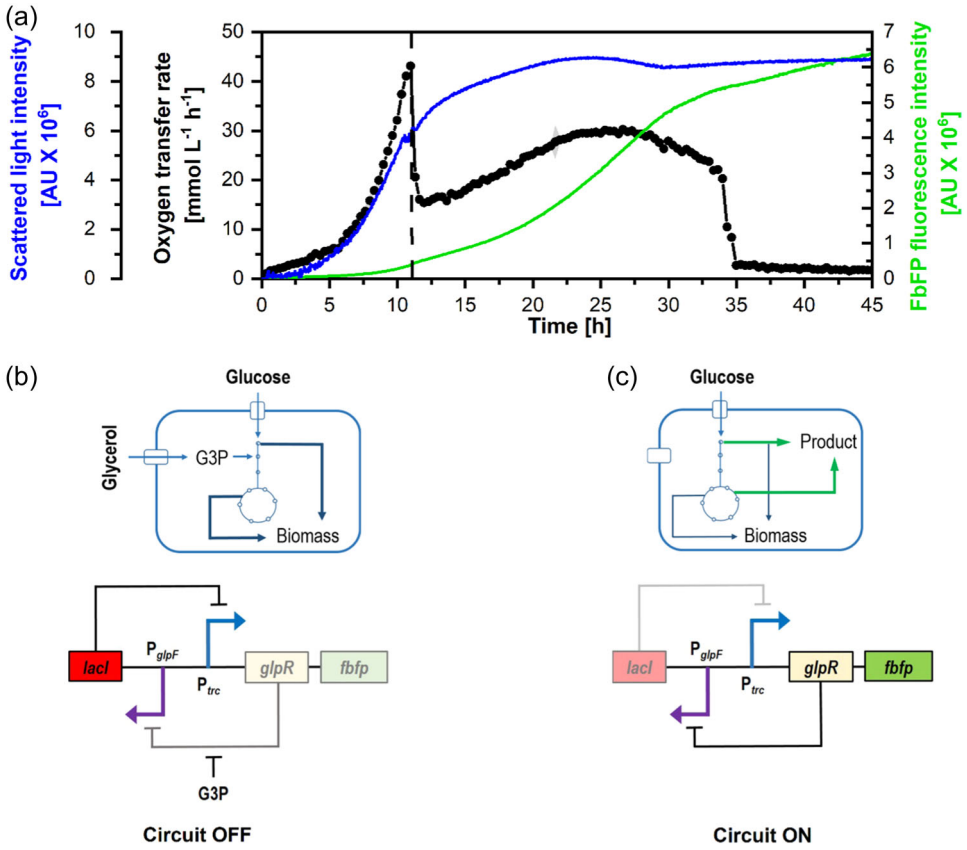

FIGURE 7 Cultures of the strain WGM bearing the GRC in 3.8 g L^{-1} glycerol + 18 g L^{-1} glucose. (a) Time course of biomass (scattered light), OTR, and FbFP fluorescence. Shaded bands indicate the standard deviation between replicates. (b) Conceptual illustration of the use of the two C-sources for biomass synthesis, while the GRC is in state OFF. (c) Conceptual illustration of the use of glucose as C-source after glycerol depletion for biomass FbFP expression, while the GRC shifts to state ON. FbFP, flavin mononucleotide-based fluorescent protein; GRC, repressible genetic circuit; OTR, oxygen transfer rates.

the GRC remains essentially OFF (Figure 7b). After glycerol depletion, both, biomass, and OTR signals slowly increased, while FbFP fluorescence increased strongly until approx. 29 h. After this point, biomass growth stagnated, and OTR decreased during approx. 5 h, until reaching a value of nearly zero. However, the FbFP fluorescence remained increasing. The SF calculated by the end of the culture reached approx. 0.70 AU AU^{-1}. This value is higher than the obtained using the CPG (Table 2). These results indicate that the shift from mixed C-sources to glucose as the only C-source in combination with the GRC allows the decoupling of the growth of the engineered strain from recombinant protein expression (Figure 7c).

Typically, the OTR falls quickly after the C-source exhaustion (Wewetzer et al., 2015). However, in cultures of strain WGM using relatively high amounts of glucose, the OTR decreased gradually before finally reaching a value close to zero (Figures 4c and 7a). Since strain WGM does not display overflow metabolism during growth in glucose (Figure 1), this cannot be associated with acetate consumption. A possible reason is the glucose affinity of the cells (K_S value). A K_S of approx. 0.5 mg L^{-1} has been reported for wild-type *E. coli* MG1655 (Smaluch et al., 2023), while the estimated K_S of strain WGM is 10 mg L^{-1} (Krausch et al., 2023). This 20-fold decreased affinity may result in a growth rate controlled by the glucose concentration at the end of the culture, which can be detected due to the relatively high cell density. However, detailed experiments are needed to clarify this behavior.

The proposed strategy combines the advantages of the engineered *E. coli* strain with the properties of the designed circuit, without any external intervention or process supervision.

4 | CONCLUSION

The glycerol-GRC in combination with the engineered *E. coli* strain and the mixture of glucose and glycerol allowed to efficiently decouple growth rate from recombinant protein expression. The system is autonomously inducible and, as demonstrated from experiments in micro and mini bioreactors, easily implemented in the laboratory. Due to the low overflow metabolism of the engineered strain, it should be possible to attain high cell densities. Therefore, the expression system proposed here, is attractive not only for early-stage product development, but also for industrial scale processes.

AUTHOR CONTRIBUTIONS

Conceptualization: Alvaro R. Lara, Juan-Carlos Sigala, Guillermo Gosset, and Jochen Büchs. *Experimental design, planning, execution, and data acquisition and analysis*: Alvaro R. Lara, Flavio Kunert, Vincent Vandenbroucke, Hilal Taymaz-Nikerel, Luz María Martínez, and Jochen Büchs. *Funding acquisition*: Alvaro R. Lara, Juan-Carlos Sigala, Guillermo Gosset, and Jochen Büchs. *Writing and review of manuscript*: all authors.

ACKNOWLEDGMENTS

This work was supported by CONAHCyT grant A1-S-8646 and the Exploratory Research Space, RWTH Aachen University.

CONFLICT OF INTEREST STATEMENT

The authors declare no conflict of interest.

DATA AVAILABILITY STATEMENT

The data that support the findings of this study are available from the corresponding author upon reasonable request.

ORCID

Alvaro R. Lara http://orcid.org/0000-0003-3535-7619
Flavio Kunert http://orcid.org/0009-0008-9297-1854
Frank Delvigne http://orcid.org/0000-0002-1679-1914
Jochen Büchs http://orcid.org/0000-0002-2012-3476

REFERENCES

Anderlei, T., & Büchs, J. (2001). Device for sterile online measurement of the oxygen transfer rate in shaking flasks. *Biochemical Engineering Journal*, *7*(2), 157–162. https://doi.org/10.1016/s1369-703x(00)00116-9

Anderlei, T., Zang, W., Papaspyrou, M., & Büchs, J. (2004). Online respiration activity measurement (OTR, CTR, RQ) in shake flasks. *Biochemical Engineering Journal*, *17*(3), 187–194. https://doi.org/10.1016/S1369-703X(03)00181-5

Borja, G. M., Meza Mora, E., Barrón, B., Gosset, G., Ramírez, O. T., & Lara, A. R. (2012). Engineering *Escherichia coli* to increase plasmid DNA production in high cell-density cultivations in batch mode. *Microbial Cell Factories*, *11*, 132. https://doi.org/10.1186/1475-2859-11-132

Bothfeld, W., Kapov, G., & Tyo, K. E. J. (2017). A glucose-sensing toggle switch for autonomous, high productivity genetic control. *ACS Synthetic Biology*, *6*(7), 1296–1304. https://doi.org/10.1021/acssynbio.6b00257

Flitsch, D., Krabbe, S., Ladner, T., Beckers, M., Schilling, J., Mahr, S., Conrath, U., Schomburg, W. K., & Büchs, J. (2016). Respiration activity monitoring system for any individual well of a 48-well microtiter plate. *Journal of Biological Engineering*, *10*, 14. https://doi.org/10.1186/s13036-016-0034-3

Fox, K. J., & Prather, K. L. (2020). Carbon catabolite repression relaxation in *Escherichia coli*: Global and sugar-specific methods for glucose and secondary sugar co-utilization. *Current Opinion in Chemical Engineering*, *30*, 9–16. https://doi.org/10.1016/j.coche.2020.05.005

Fragoso-Jiménez, J. C., Gutierrez-Rios, R. M., Flores, N., Martinez, A., Lara, A. R., Delvigne, F., & Gosset, G. (2022). Glucose consumption rate-dependent transcriptome profiling of *Escherichia coli* provides insight on performance as microbial factories. *Microbial Cell Factories*, *21*, 189. https://doi.org/10.1186/s12934-022-01909-y

Fuentes, L. G., Lara, A. R., Martínez, L. M., Ramírez, O. T., Martínez, A., Bolívar, F., & Gosset, G. (2013). Modification of glucose import capacity in *Escherichia coli*: Physiologic consequences and utility for improving DNA vaccine production. *Microbial Cell Factories*, *12*, 42. https://doi.org/10.1186/1475-2859-12-42

Gardner, T. S., Cantor, C. R., & Collins, J. J. (2000). Construction of a genetic toggle switch in *Escherichia coli*. *Nature*, *403*(6767), 339–342. https://doi.org/10.1038/35002131

Gonzalez, R., Murarka, A., Dharmadi, Y., & Yazdani, S. S. (2008). A new model for the anaerobic fermentation of glycerol in enteric bacteria: Trunk and auxiliary pathways in *Escherichia coli*. *Metabolic Engineering*, *10*(5), 234–245. https://doi.org/10.1016/j.ymben.2008.05.001

Guo, Q., Ullah, I., Zheng, L. J., Gao, X. Q., Liu, C. Y., Zheng, H. D., Fan, L. H., & Deng, L. (2022). Intelligent self-control of carbon metabolic flux in SecY-engineered *Escherichia coli* for xylitol biosynthesis from xylose-glucose mixtures. *Biotechnology and Bioengineering*, *119*(2), 388–398. https://doi.org/10.1002/bit.28002

Hemm, M. R., Paul, B. J., Miranda-Ríos, J., Zhang, A., Soltanzad, N., & Storz, G. (2010). Small stress response proteins in *Escherichia coli*: Proteins missed by classical proteomic studies. *Journal of Bacteriology*, *192*(1), 46–58. https://doi.org/10.1128/JB.00872-09

Henrion, L., Martinez, J. A., Vandenbroucke, V., Delvenne, M., Telek, S., Zicler, A., Grünberger, A., & Delvigne, F. (2023). Fitness cost associated with cell phenotypic switching drives population diversification dynamics and controllability. *Nature Communications*, *14*(1), 6128. https://doi.org/10.1038/s41467-023-41917-z

Kasari, M., Kasari, V., Kärmas, M., & Jõers, A. (2022). Decoupling growth and production by removing the origin of replication from a bacterial chromosome. *ACS Synthetic Biology*, *11*(8), 2610–2622. https://doi.org/10.1021/acssynbio.1c00618

Krausch, N., Kaspersetz, L., Gaytán-Castro, R. D., Schermeyer, M.-T., Lara, A. R., Gosset, G., Cruz Bournazou, M. N., & Neubauer, P. (2023). Model-based characterization of *E. coli* strains with impaired glucose uptake. *Bioengineering*, *10*, 808. https://doi.org/10.3390/bioengineering10070808

Ladner, T., Held, M., Flitsch, D., Beckers, M., & Büchs, J. (2016). Quasi-continuous parallel online scattered light, fluorescence and dissolved oxygen tension measurement combined with monitoring of the oxygen transfer rate in each well of a shaken microtiter plate. *Microbial Cell Factories*, *15*(1), 206. https://doi.org/10.1186/s12934-016-0608-2

Lara, A. R., Caspeta, L., Gosset, G., Bolívar, F., & Ramírez, O. T. (2008). Utility of an *Escherichia coli* strain engineered in the substrate uptake system for improved culture performance at high glucose and cell concentrations: An alternative to fed-batch cultures. *Biotechnology and Bioengineering*, *99*(4), 893–901. https://doi.org/10.1002/bit.21664

Lara, A. R., Galindo, E., Ramírez, O. T., & Palomares, L. A. (2006). Living with heterogeneities in bioreactors: Understanding the effects of environmental gradients on cells. *Molecular Biotechnology*, *34*(3), 355–382. https://doi.org/10.1385/MB:34:3:355

Lara, A. R., Jaén, K. E., Sigala, J. C., Mühlmann, M., Regestein, L., & Büchs, J. (2017). Characterization of endogenous and reduced promoters for oxygen-limited processes using *Escherichia coli*. *ACS Synthetic Biology*, *6*(2), 344–356. https://doi.org/10.1021/acssynbio.6b00233

Lara, A. R., Jaén, K. E., Sigala, J. C., Regestein, L., & Büchs, J. (2017). Evaluation of microbial globin promoters for oxygen-limited processes using *Escherichia coli*. *Journal of Biological Engineering*, *11*, 39. https://doi.org/10.1186/s13036-017-0082-3

Lin, E. C. C. (1976). Glycerol dissimilation and its regulation in bacteria. *Annual Review of Microbiology*, *30*, 535–578. https://doi.org/10.1146/annurev.mi.30.100176.002535

Li, Z., Kessler, W., van den Heuvel, J., & Rinas, U. (2011). Simple defined autoinduction medium for high-level recombinant protein production using T7-based *Escherichia coli* expression systems. *Applied Microbiology and Biotechnology*, *91*(4), 1203–1213. https://doi.org/10.1007/s00253-011-3407-z

Lo, T. M., Chng, S. H., Teo, W. S., Cho, H. S., & Chang, M. W. (2016). A two-layer gene circuit for decoupling cell growth from metabolite production. *Cell Systems*, *3*(2), 133–143. https://doi.org/10.1016/j.cels.2016.07.012

Martínez, K., de Anda, R., Hernández, G., Escalante, A., Gosset, G., Ramírez, O. T., & Bolívar, F. G. (2008). Coutilization of glucose and glycerol enhances the production of aromatic compounds in an *Escherichia coli* strain lacking the phosphoenolpyruvate: Carbohydrate phosphotransferase system. *Microbial Cell Factories*, *7*, 1. https://doi.org/10.1186/1475-2859-7-1

Martínez-Gómez, K., Flores, N., Castañeda, H. M., Martínez-Batallar, G., Hernández-Chávez, G., Ramírez, O. T., Gosset, G., Encarnación, S., & Bolivar, F. (2012). New insights into *Escherichia coli* metabolism: Carbon scavenging, acetate metabolism and carbon recycling responses during growth on glycerol. *Microbial Cell Factories*, *11*, 46. https://doi.org/10.1186/1475-2859-11-46

Menacho-Melgar, R., Ye, Z., Moreb, E. A., Yang, T., Efromson, J. P., Decker, J. S., Wang, R., & Lynch, M. D. (2020). Scalable, two-stage, autoinduction of recombinant protein expression in *E. coli* utilizing phosphate depletion. *Biotechnology and Bioengineering*, *117*(9), 2715–2727. https://doi.org/10.1002/bit.27440

Okano, H., Hermsen, R., Kochanowski, K., & Hwa, T. (2020). Regulation underlying hierarchical and simultaneous utilization of carbon substrates by flux sensors in *Escherichia coli*. *Nature Microbiology*, *5*(1), 206–215. https://doi.org/10.1038/s41564-019-0610-7

Orth, J. D., Conrad, T. M., Na, J., Lerman, J. A., Nam, H., Feist, A. M., & Palsson, B. Ø. (2011). A comprehensive genome-scale reconstruction of *Escherichia coli* metabolism. *Molecular Systems Biology*, *7*, 535.

Sassi, H., Nguyen, T. M., Telek, S., Gosset, G., Grünberger, A., & Delvigne, F. (2019). Segregostat: A novel concept to control phenotypic diversification dynamics on the example of Gram-negative bacteria. *Microbial Biotechnology*, *12*(5), 1064–1075. https://doi.org/10.1111/1751-7915.13442

Schellenberger, J., Que, R., Fleming, R. M. T., Thiele, I., Orth, J. D., Feist, A. M., Zielinski, D. C., Bordbar, A., Lewis, N. E., Rahmanian, S., Kang, J., Hyduke, D. R., & Palsson, B. Ø. (2011). Quantitative prediction of cellular metabolism with constraint-based models: The COBRA Toolbox v2.0. *Nature Protocols*, *6*, 1290–1307.

Smaluch, K., Wollenhaupt, B., Steinhoff, H., Kohlheyer, D., Grünberger, A., & Dusny, C. (2023). Assessing the growth kinetics and stoichiometry of *Escherichia coli* at the single-cell level. *Engineering in Life Sciences*, *23*(1), e2100157. https://doi.org/10.1002/elsc.202100157

Stargardt, P., Feuchtenhofer, L., Cserjan-Puschmann, M., Striedner, G., & Mairhofer, J. (2020). Bacteriophage inspired growth-decoupled recombinant protein production in *Escherichia coli*. *ACS Synthetic Biology*, *9*(6), 1336–1348. https://doi.org/10.1021/acssynbio.0c00028

Strittmatter, T., Argast, P., Buchman, P., Krawczyk, K., & Fussenegger, M. (2021). Control of gene expression in engineered mammalian cells with a programmable shear-stress inducer. *Biotechnology and Bioengineering*, *118*(12), 4751–4759. https://doi.org/10.1002/bit.27939

Strittmatter, T., Egli, S., Bertschi, A., Plieninger, R., Bojar, D., Xie, M., & Fussenegger, M. (2021). Gene switch for l-glucose-induced biopharmaceutical production in mammalian cells. *Biotechnology and Bioengineering*, *118*(6), 2220–2233. https://doi.org/10.1002/bit.27730

Studier, F. W. (2005). Protein production by auto-induction in high density shaking cultures. *Protein Expression and Purification*, *41*(1), 207–234. https://doi.org/10.1016/j.pep.2005.01.016

Taymaz-Nikerel, H., & Lara, A. R. (2021). *Vitreoscilla* haemoglobin: A tool to reduce overflow metabolism. *Microorganisms*, *10*(1), 43. https://doi.org/10.3390/microorganisms10010043

Velazquez, D., Sigala, J. C., Martínez, L. M., Gaytán, P., Gosset, G., & Lara, A. R. (2022). Glucose transport engineering allows mimicking fed-batch performance in batch mode and selection of superior producer strains. *Microbial Cell Factories*, *21*, 183. https://doi.org/10.1186/s12934-022-01906-1

Werner, N. S., Weber, W., Fussenegger, M., & Geisse, S. (2007). A gas-inducible expression system in HEK.EBNA cells applied to controlled proliferation studies by expression of p27(Kip1). *Biotechnology and Bioengineering*, *96*(6), 1155–1166. https://doi.org/10.1002/bit.21235

Wewetzer, S. J., Kunze, M., Ladner, T., Luchterhand, B., Roth, S., Rahmen, N., Kloß, R., Costa e Silva, A., Regestein, L., & Büchs, J. (2015). Parallel use of shake flask and microtiter plate online measuring devices (RAMOS and BioLector) reduces the number of experiments in laboratory-scale stirred tank bioreactors. *Journal of Biological Engineering*, *9*, 9. https://doi.org/10.1186/s13036-015-0005-0

Yao, R., Xiong, D., Hu, H., Wakayama, M., Yu, W., Zhang, X., & Shimizu, K. (2016). Elucidation of the co-metabolism of glycerol and glucose in *Escherichia coli* by genetic engineering, transcription profiling, and ^{13}C metabolic flux analysis. *Biotechnology for Biofuels*, *9*, 175. https://doi.org/10.1186/s13068-016-0591-1

You, C., Okano, H., Hui, S., Zhang, Z., Kim, M., Gunderson, C. W., Wang, Y. P., Lenz, P., Yan, D., & Hwa, T. (2013). Coordination of bacterial proteome with metabolism by cyclic AMP signalling. *Nature*, *500*(7462), 301–306. https://doi.org/10.1038/nature12446

SUPPORTING INFORMATION

Additional supporting information can be found online in the Supporting Information section at the end of this article.

How to cite this article: Lara, A. R., Kunert, F., Vandenbroucke, V., Taymaz-Nikerel, H., Martínez, L. M., Sigala, J.-C., Delvigne, F., Gosset, G., & Büchs, J. (2024). Transport-controlled growth decoupling for self-induced protein expression with a glycerol-repressible genetic circuit. *Biotechnology and Bioengineering*, 1–14. https://doi.org/10.1002/bit.28697